Int J Energy Environ Eng (2017) 8:9–23
DOI 10.1007/s40095-016-0226-0

ORIGINAL RESEARCH

Biodiesel from rapeseed oil (*Brassica napus*) by supported Li_2O and MgO

Jerry L. Solis[1,2,3] · Albin L. Berkemar[3] · Lucio Alejo[1] · Yohannes Kiros[3]

Received: 9 September 2016 / Accepted: 14 December 2016 / Published online: 23 December 2016

Abstract Vegetable oils are a vast triglyceride source for biodiesel production; i.e. fatty acid methyl esters (FAME), with methanol and a catalyst via transesterification reaction. The aim of this work was to study heterogeneously catalysed biodiesel production with solid oxides such as mayenite ($Ca_{12}Al_{14}O_{33}$) and alumina (Al_2O_3) as catalyst carriers using edible rapeseed oil as feedstock. These oxides were impregnated to have Li_2O and MgO concentrations of 5–10 and 5–30 wt% on each carrier, respectively. The catalysts were characterized using N_2-physisorption (BET/BJH), scanning electron microscopy (SEM), and X-ray diffraction (XRD) analyses. The synthesized catalysts were mesoporous ranging from 119 to 401 Å and their chemical phase composition was confirmed by the XRD. The catalyst coating (MgO/Li_2O) was studied, along with the catalyst amount in the reactor and the assessment of the transesterification reaction kinetics. The reaction was studied at 60 °C, atmospheric pressure, agitation rate of 180 rpm, and a reaction time of 2 h in a 6:1 molar ratio of methanol to oil. For each catalyst, loadings of 2.5, 5, and 10 wt% relative to the oil weight were evaluated. The highest biodiesel yield was obtained by 5 wt% (relative to oil weight) impregnated mayenite catalyst coated with 10 wt% of Li_2O. The kinetic data fits to a pseudo-first-order model having a reaction rate constant equal to 0.045 min^{-1} under these mild reaction conditions.

Keywords Biodiesel · Transesterification · Heterogeneous catalyst · Mayenite · Alumina, MgO, Li_2O

Introduction

Vegetable oils (triglycerides) feedstock and market are affected by several factors; e.g. population growth expressed through supply and demand, biodiesel access rate and production, and fossil oil price fluctuations. Among the adversities of biodiesel production are the lower prices of petroleum barrel, which reduces the biodiesel production cost advantage (no competitive cost) and the food security policies that disregard integrated food-biofuel policies to boost biofuel production [1, 2]. Despite such adversities, worldwide biodiesel production from vegetable oils is constantly growing [3, 4]. Broad availability of vegetable oils has made biodiesel (BD) production from these feedstocks (first generation) to be well-known and optimized processes, which are commercialized in many parts of the world [5–7].

Even though vegetable oil production is increasing [8], the driving force towards eco-friendly biofuels has changed the attention towards second and third generation feedstocks; i.e. non-edible oils, waste cooking oil, animal fats and algae. Algae was first regarded as a second generation feedstock but as it showed higher oil production yields with lower resource inputs than other feedstock, it was placed as a third generation feedstock. Oil yield of algae is higher than soybean oil and rapeseed oil by 130 times and 50 times, respectively [9–11].

✉ Jerry L. Solis
jlsv2@kth.se

[1] Centro de Tecnología Agroindustrial, FCyT, UMSS Universidad Mayor de San Simón, Cochabamba, Bolivia

[2] Centro de Biotecnología, FCyT Universidad Mayor de San Simón, Cochabamba, Bolivia

[3] Department of Chemical Engineering and Technology, KTH Royal Institute of Technology, 100 44 Stockholm, Sweden

Micro-emulsions, thermal cracking and transesterification have been proven to reduce the use of fossil fuel and achieve a vegetable oil-based biofuel [12]. Renewability, high cetane number, lower emissions, and higher combustion efficiency are the advantages of transesterification over the other BD production methods [13]. In transesterification, triglycerides are separated to glycerol and fatty acid-alkyl esters (FAAE) with alcohol as a reactant and a catalyst. Under homogeneous reaction conditions, the reaction mixtures (containing BD, alcohol, catalyst, waste water, and glycerol) have to undergo a series of purification, separation, and final disposal processes, which are the drawbacks in high-scale BD production. Even though homogeneous transesterification has high reaction rates, non-reusability of the catalyst and further downstream process hinders the economic competitiveness with respect to fossil diesel [14].

Different catalysts and feedstocks were used to overcome BD production restraints, along with the reaction conditions such as temperature, catalyst loading and alcohol to oil molar ratio [12, 15, 16]. Heterogeneous, enzymatic and even with supercritical reactant (alcohol) transesterifications have been studied as alternatives to improve BD production. Heterogeneously produced BD studies have increased as the preferred transesterification method, since it is environmentally benign, needs no water-washing and product separation is much easier [17, 18]. Different feedstocks, from non-edible oils [19, 20] to algae [11, 21], have also been tested for BD production. However, BD production with such feedstocks is challenging due to high free fatty acid (FFA) contents and water presence [15]. FFAs and water have a negative effect over alkali catalysed transesterification. Soap formation has been reported among the negative effects, followed by deactivation of the catalyst [10, 22, 23]. As a result, developing a high activity heterogeneous catalyst despite the FFA content and water content has become a challenge [24, 25].

The catalysts for transesterification must have a support that can hold the reactive oxides, being stable and compatible with the active material to be adsorbed. Some of the most used supports found in literature include aluminium, zirconium and titanium oxides, ferromagnetic nanoparticles, mesoporous silica, ion-exchange resins, and zeolites [26]. These supports might have some active sites which increase the yields of the BD production. Under the support requirements listed above, alumina and mayenite are good candidates for catalyst support. Alumina (Al_2O_3) is a widely used mineral, as a catalyst and as a catalyst support, due to its favourable properties; e.g. structural and chemical properties [27, 28]. Alumina is a strong Lewis acid, specifically the tetrahedral aluminium sites. Among the applications of alumina are Fischer–Tropsch synthesis (FTS), dimethyl ether catalysed production [29], and partial hydrogenation of hydrocarbon based fuels [30]. Alumina has been studied as heterogeneous catalyst for BD production by several authors [31–36], using mild transesterification conditions such as 60 °C, atmospheric pressure, and mixing rates of 250 rpm. Mayenite ($Ca_{12}Al_{14}O_{33}$) is a mineral common in high-temperature, thermally metamorphosed, impure limestone included in volcanic rocks [37]. Applications of mayenite as a material include its use as a transparent conductive oxide (TCO), as a catalyst for the combustion of volatile organic compounds (VOC) or as an ionic conductor [38]. Catalytic hydrogenation, steam reforming, and catalysed transesterification using mayenite as the catalyst support have also been reported [39–42] showing the suitability of such material as a desired support in the formulation of a novel catalyst for transesterification reaction promotion.

Alkali and alkaline earth metal oxides have been extensively tested as catalytically active phases for heterogeneous transesterification of triglycerides [43–46]. Lithium and magnesium oxides—from the alkali metal and the alkaline earth metal groups, respectively—have been proven to be dominant catalysts due to their physical and chemical properties. Lithium oxide surpasses the other oxides of its group due its high catalytic activity, crystallite ordering effect, and high basic strength, which are advantageous properties for vegetable oil heterogeneous transesterification [47]. Biodiesel production was achieved with this element in mixed oxides [48, 49] and over different supports [34, 50]. Magnesium oxide catalysts have also been studied (as the active phase and as a catalyst support) and it is reported to be vastly active towards transesterification reactions. Depending on the support and the magnesium species involved some variations of the catalytic capability have been reported [46, 51, 52]. Such differences might happen due to several variables such as synthesizing conditions in the calcination procedure and the precursors used. To prepare the catalyst for the transesterification reaction, lithium and magnesium oxides were impregnated over the supports, as they were reported to be catalytically active and suitable to be adsorbed on supports to be used in transesterification reactions [18].

Several reaction conditions are considered in heterogeneous catalysed BD production, among them are reaction temperature, agitation rate, methanol to oil molar ratio, catalyst loading, etc. [13, 26, 53]. Different authors presented high BD yields with high temperatures [54] and long reaction times [55], but the present study focused in BD production at rather mild conditions (low temperature and short reaction times). Temperature is an important factor as its increase or decrease affects the reaction yield [56–58] and will also affect the reaction time and agitation rate [59]. If a catalyst is weakly promoting the

transesterification reaction, higher reaction temperatures will be needed to carry the reactants through the transesterification reaction. In low activity catalyst conditions, agitation rate or reaction times are affected negatively, resulting in the need of higher mixing agitation rates or longer reaction times [59]. In contrast, transesterification studies reported by Boz and Kara [55] and Endalew et al. [25], among others, show high BD yields working at 60 °C with improved solid catalysts. The reaction time was set to reach the maximum possible conversion in 2 h as reported in other studies for heterogeneously catalysed systems [60]. Agitation rate reported range is quite wide, depending on the transesterification study for homogeneous or heterogeneous catalysts, the agitation may vary from 1200 rpm [61] to 100 rpm [62], respectively. Finally, the methanol to oil molar ratios determines the yield of the transesterification reaction. Reported data shows a variation ranging from 6:1 to even 30:1 [15, 54], meaning a fivefold requirement of methanol compared to other reaction setups. The molar ratio of methanol used has to be more than the stoichiometrically needed and it has been proved to be useful at least at a 6:1 molar ratio related to oil to achieve biodiesel production [12, 15]. In this study, we kept that ratio to decrease the effects of over using such reactant.

The present work deals with the preparation and application of catalysts, which are found to be effective for the transesterification of rapeseed oil by solid oxides. The catalysts made of a stable support (synthesized mayenite or commercial alumina) and a highly active phase (Li_2O or MgO) were used to produce biodiesel at low energy consumption and reactant use as possible compared to literature. Translated to reaction conditions, the reaction temperature was 60 °C with an agitation rate of 180 rpm. In terms of reactant use, the methanol to oil molar ratio was kept low at 6:1 for all the experiments. The best catalysts were chosen afterwards to analyse the kinetics of the BD production and their reusability potential.

Materials and methods

Materials

Commercial refined rapeseed oil from the brand Zeta was used, along with methanol puriss p.a. (≥99.8% GC, Sigma-Aldrich), aluminium nitrate nonahydrate ACS (≥98.0%, Sigma-Aldrich), lithium hydroxide monohydrate ACS (≥98.0%, Sigma-Aldrich), isopropyl alcohol (≥99.7% FCC, Sigma-Aldrich), calcium hydroxide ACS (≥95.0%, Sigma-Aldrich), magnesium acetate tetrahydrate p.a. (≥99.0% GC, Fluka), propyl acetate (≥96.0% GC, Fluka), alumina pellets (Norton 1/16″), and *n*-heptane (≥99.0% HPLC, Carlo Erba reactifs) were used for the present study.

Synthesis of the support and catalyst

Alumina based catalysts

To prepare alumina-supported catalysts (Li_2O/Al_2O_3 and MgO/Al_2O_3), alumina (Al_2O_3) was dried at 100 °C until the weight of the sample remained constant, then it was cooled to room temperature. Lithium hydroxide and magnesium acetate were then separately dissolved in methanol. The dissolved salts were then soaked in Al_2O_3 in weight proportions to achieve 5–10 wt% Li_2O (A_1 and A_2) and 5–30 wt% MgO (A_3, A_4, and A_5) on the support. The mixtures were dried at 100 °C overnight, calcined at 650 °C for 2 h, cooled down and stored for further use.

Mayenite based catalysts

Mayenite support was produced by mixing stoichiometric amounts of calcium hydroxide and aluminium nitrate. Isopropanol was added when slurry was formed and it was heated up to 80 °C until the mixture was clear, then it was taken to the oven to be dried at 100 °C. After 72 h drying process, the mixture was milled in a mortar and calcinated at 650 °C for 2 h. At the end of calcination the produced mayenite was cooled down and mixed with the catalytic material as in the alumina impregnation described above to produce mayenite-Li_2O and mayenite-MgO catalysts, with 5–10 and 5–30 wt% of impregnated oxides, respectively. Mayenite-supported catalysts were also named and numbered after the support in increasing order from M_0 (bare mayenite), M_1–M_2 (lithium impregnated mayenite), and M_3–M_4 (magnesium impregnated mayenite).

Characterization of the support/catalyst

Characterization of the support/catalyst morphology was performed using Zeiss Ultra 55 scanning electron microscopy (SEM) in the range of 1 μm to 200 nm. Determination of the support/catalyst porosity, pore volume, and surface area were determined using a Micromeritics ASAP 2000 N_2-physisorption apparatus. The catalyst samples were degassed at a temperature of 523 K for approximately 5 h. The adsorption isotherms were carried out at a temperature of 77 K to perform BJH and BET analyses. X-ray diffraction analyses were also performed with a Siemens diffractometer D5000 using Cu-Kα radiation source ($\lambda = 1.5406$ Å) in a 2θ degree range from 20° to 80°. The diffractograms were analysed with EVA software and the identification of the chemical species was performed correlating the data to powder diffraction file (PDF) numbers.

Transesterification and product characterization

The transesterification of rapeseed oil was performed in a round-bottom flask reactor that included a thermometer, a magnetic stirrer and a condenser. Methanol and rapeseed oil (6:1 molar ratio) were mixed in the reactor with the catalyst loadings of 5 wt% (relative to oil mass) at 180 rpm, 60 °C, and atmospheric pressure for 2 h. After the end of the reaction the mixture was transferred into a graduated cylinder and left to settle down for the separation of the liquid phases.

Transesterification samples were analysed with gas chromatography (Agilent GC 6890) using a capillary column (HP-FFAP polyethylene glycol 30 m × 530 μm × I.D. 1 μm) at a temperature of 215 °C with helium at 7.2 mL/min as the carrier phase and a split ratio of 80:1. The GC is equipped with a flame detector ionization detector (FID) working at 300 °C. The samples were prepared by taking 113 μL from the FAME phase, mixed with 11 μL of propyl acetate (as the internal standard) and 500 μL *n*-heptane (as the solvent). The quantification of biodiesel yield was elaborated by fitting the results in a standard curve made with different solutions containing a FAME standard of known concentration.

Impregnation amount and catalyst concentration effects in BD production

The experiments to test the potential use of the produced catalysts were carried with the catalysts with different Li_2O or MgO impregnated amounts over the supports (alumina or mayenite). The transesterifications were performed for each catalyst at the experimental conditions described above and a fixed catalyst concentration of 5 wt% relative to oil mass as the results were recorded and further used in the following steps. Afterwards, all the catalysts were used in different concentrations for the transesterification reaction to observe the effects of the catalyst concentration. The concentration range of the catalysts that were tested included 2.5, 5.0, and 10.0 wt% of catalyst relative to oil mass (excluding A_0 and M_0). All the remaining reaction conditions were kept as indicated above.

Transesterification kinetics

Kinetic studies were carried out on the transesterification reaction using the catalyst with the highest biodiesel yield. The experimental setup was the same as in section 2.4 and 1 mL samples were taken with glass Pasteur pipettes every 20 min from the core of the reactor during 2 h of reaction time. The samples were left to settle down and taken for GC analysis to determine their FAME content.

Catalyst reuse potential

Two catalysts were selected based on their activity inferred from their BD production yields. The reuse capability was studied for a second use of such catalysts after a cycle of reaction; i.e. an experimental run using 5.0 wt% of such catalysts with a 6:1 methanol to oil molar ratio, an agitation rate of 180 rpm, a temperature of 60 °C, and atmospheric pressure for 2 h of reaction time. The mixture was transferred to a graduated cylinder to settle down. After the formation of the different component phases—catalyst, glycerol, biodiesel, and methanol—the catalyst was separated, filtered, and washed with CH_3OH. Once the catalyst was separated from glycerol, the second cycle of transesterification under the same conditions was performed.

Results and discussion

Characterization of the support/catalysts

Alumina and mayenite were characterized for their ability as support materials. Li_2O and MgO were impregnated as active phase on the supports to have a total of nine catalysts, which had BET specific surfaces, pore volumes, and pore diameters, as shown in Table 1.

BET analyses reveal small surface areas on mayenite-derived catalysts, as reported by Li et al. [63] and Ruszak et al. [64], having surface areas of 1 and 5 m^2g^{-1}, respectively. The impregnation of Li_2O and MgO notably show an increased surface area, more than ten times in the best case (M_4). In addition to a larger surface area, Li_2O impregnation increases pore diameter and pore volume of the mayenite-derived catalysts compared to bare mayenite. Such advantageous properties enhance the catalytic activity in two possible ways. First, the large pore volumes provide more room to large triglyceride molecules to reach the active sites and proceed to adsorption (increased pore diffusion). The second improvement is that the catalyst has more adsorption area for the methoxy complex and the triglyceride-catalyst complex to form and react through the transesterification mechanism [65]. Such desired properties are seen and confirmed by the larger biodiesel yield when the reaction is carried with the catalyst M_2. The impregnation of MgO on mayenite increases the surface areas and pore volume (M_3 and M_4) but the increase of the pore diameter is smaller compared to the Li_2O impregnation case, which may alter the accessibility to the active sites.

On the other hand, alumina surface properties, e.g. surface area and pore volume, are larger than mayenite, as shown in Table 1. High surface area of 102 m^2g^{-1} and 650 °C calcination temperature suggests that alumina might be in gamma phase [66]. The effect of Li_2O and

Table 1 Surface properties of the synthesized catalysts

Catalyst type	Support	Catalytic additive[a]	BET m^2g^{-1}	Pore D[b] Å	Pore V[c] cm^3g^{-1}
A_0	Alumina	–	102	181	0.464
A_1	Alumina	5% Li_2O	79.2	183	0.363
A_2	Alumina	10% Li_2O	68.4	176	0.300
A_3	Alumina	5% MgO	86.9	175	0.381
A_4	Alumina	30% MgO	77.3	165	0.320
A_5	Alumina	30% MgO and lumps	76.0	178	0.340
M_0	Mayenite	–	1.85	267	0.012
M_1	Mayenite	5% Li_2O	9.46	297	0.078
M_2	Mayenite	10% Li_2O	15.2	401	0.170
M_3	Mayenite	5% MgO	7.61	181	0.038
M_4	Mayenite	30% MgO	21.2	119	0.072

[a] The additives are Li2O or MgO impregnated on the support in wt%

[b] D stands for pore diameter

[c] V stands for pore volume

MgO wet impregnation over alumina reduced to an extent such properties. Despite alumina-supported catalyst showed reduction of surface areas compared to bare alumina, pore volumes are still larger than mayenite-supported catalysts offering more space for reactants to access the active sites.

The prepared catalysts and bare supports without impregnation were analysed by powder XRD from 20.0 to 80.0 2θ angles. XRD diffractogram shows peaks at 32.5°, 37.2°, 46.0°, corresponding to alumina (Al_2O_3 PDF-01-074-4629) [67, 68]. Figure 1 shows the complete set of diffractograms for alumina-derived catalysts.

Regarding Li_2O-alumina catalysts (A_0, A_1, and A_2), not only characteristic peaks of Li_2O are present (PDF-00-012-0254 $2\theta = 33.5°$, 38.2°, 67.0°) [69] but also peaks that suggest the presence of the specie lithium aluminate ($LiAlO_2$ PDF-01-073-1338) [70, 71] are found in the A_2 diffractogram. Lithium aluminate has three allotropic forms [72], two of which—γ-$LiAlO_2$ and β-$LiAlO_2$—have signals at 22.3°, 23.3°, 28.8°, 34.1°, 50.5°, 58.8° and 60.4° [70]. The preparation method was successful in the adsorption of Li_2O on alumina surface but also in the formation of $LiAlO_2$ species. The formation of this species stabilizes the material, improving its reuse potential.

In the case of MgO impregnation over alumina (A_3, A_4, and A_5), the most intense signal is caused by cubic MgO formation at high concentration (30 wt%), showing high signals at 43.0° and 62.0° (PDF-01-071-1176). Characteristic peaks of orthorhombic magnesium aluminate spinel ($MgAl_2O_4$ PDF-00-033-0853) are also shown in the diffractogram A_4 and A_5, which show signals at 28.2°, 32.2°, and 43.0°. Magnesium spinel powders are advantageous due to chemical stability and resistance, and chemical inertness [73, 74].

Mayenite XRD diffractogram signal (M_0) in Figs. 2 and 3 shows peaks at 24.0°, 31.2°, 34.0, 37.8°, and 54.2° (PDF-00-009-0413). Mayenite-supported catalyst XRD diffractograms (M_1 and M_2) show that Li_2O and MgO were not only adsorbed on the mayenite structure but also show that other species have been formed, such as tetragonal $LiAlO_2$ (PDF-01-073-1338 $2\theta = 35.0°$, 45.4°, 61.6°) and orthorhombic Li_5AlO_4 (PDF-00-024-0596 $2\theta = 22.7°$, 37.8°, 45.7°). The diffractograms of the catalysts M_0, M_1, and M_2 show that the increase of lithium (0, 5, and 10 wt%) induces the formation of the specie Li_5AlO_4 (PDF-01-071-1736 $2\theta = 32.1°$, 37.7°, 45.9°, 67.1°) by the increase of the signal at 37.7°. Characteristic peaks of cubic CaO are also present at 32.5, 37.5, 54.8, 64.3, and 67.6° (PDF-01-070-5490). The M_1 catalyst diffractogram also suggests the presence of $CaCO_3$ by the characteristic signals at 29.8° and 39.6°, which might emanate from CO_2 in the air during calcination.

A cubic MgO phase found over mayenite catalysts was identified by the peaks at 37.2°, 43.3°, and 62.7° (PDF 01-071-1176) in the M_3 and M_4 diffractograms in Fig. 3. The diffractograms M_3 and M_4 show that not only a phase of MgO over mayenite support was successfully achieved but also shows that some magnesium aluminate ($MgAl_2O_4$ PDF-00-033-0853) has been formed over mayenite. The diffractogram shown in Fig. 3 confirm that the major components of the catalysts M_3 and M_4 are MgO and mayenite. The formation of additional compounds might be a result of contact with the atmosphere, impurities from the initial reagents, and the conditions of the catalyst preparation; e.g. temperature and atmosphere in the oven.

In addition to N_2-physisorption and XRD characterization procedures, SEM micrographs were performed on samples of the catalysts to determine the particle

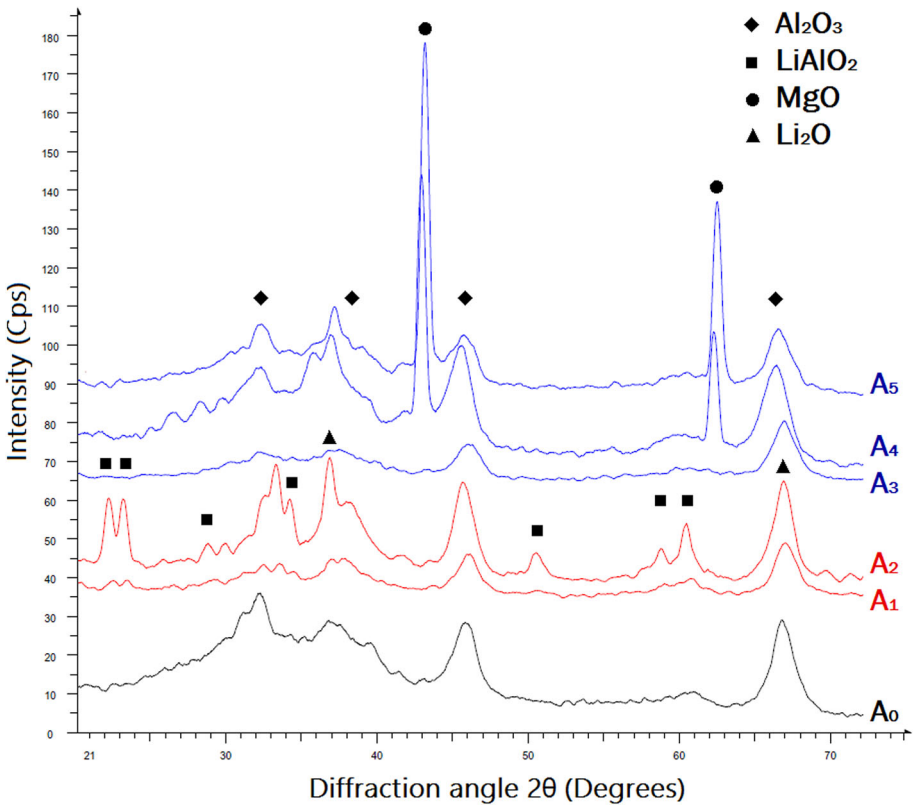

Fig. 1 XRD diffractograms of alumina-supported catalysts

morphology. The SEM micrographs of mayenite show that its particles have a rectangular and intertwined agglomerate with an average size of 266 nm and varying cavities between 20 and 180 nm (Fig. 4a). Mayenite impregnated with 5 wt% of Li_2O presented lotus-like formations (Fig. 4b), crisscrossing the surface with shallow holes.

In contrast, alumina SEM micrographs show a cloudy-like agglomeration of γ-alumina (Fig. 5a). Li_2O seems to give more order to the alumina surface but still shows that no specific shape can be the attribute of its particles (Fig. 5b). Finally, MgO over alumina micrograph (Fig. 5c) suggests amorphous formation on the alumina catalysts that were impregnated with MgO (A_3, A_4, and A_5). Due to the amorphous nature of the alumina-derived catalyst particles, it was not possible to have an average particle size.

Impregnation effect in transesterification

The prepared catalysts were used for the biodiesel production tests, where the supports without impregnation of active phase were used as control samples (M_0 and A_0). The assessment of the catalyst effect per oil mass on FAME yields was performed on several batches using each different catalyst batchwise (Figs. 6, 7).

The fact that alumina is slightly catalytic for the transesterification becomes evident when observing Fig. 6 reaching 14.0% of BD yield. In the case of lithium oxide impregnation, the experiments showed that an increase of lithium oxide concentration on the support reduced the BD yield. The composition increase from 5.0 to 10 wt% of Li_2O on the alumina support was followed by a reduction of 13% BD yield (relatively comparing A_1 and A_2 BD yields in Fig. 6). It is apparent that the presence of Li_2O and Al_2O_3 in the surface of catalyst A_1 has higher catalytic activity than the $LiAlO_2$ specie found in the catalyst A_2, as shown in the XRD analysis in Fig. 2. This further suggests that the basic nature of the Li_2O and the acidic nature of the Al_2O_3 interaction increase the catalysts activity more than the formation of the stabilized structure of $LiAlO_2$, as well as the reduction of the available surface area and pore volume, which increases the mass transfer limitations towards the formation of the transesterification intermediates [65].

When impregnating the alumina with MgO (A_3, A_4 and A_5), the BD production reaches a yield of 84.3% (catalyst A_3 shown in Fig. 6). The same hindrance to the reaction yield at the higher impregnation concentration appears again for the case of the MgO impregnated catalysts (from the catalyst A_3 to A_4), at higher MgO concentration (A_4) the BD yield decreases to 83.4%. Considering bare alumina activity, the BD overall yields might be achieved by the simultaneous action of alumina (acidic) and magnesium oxide (basic) but it is clear that the formation of different oxide species, such as $MgAl_2O_4$ as determined by XRD

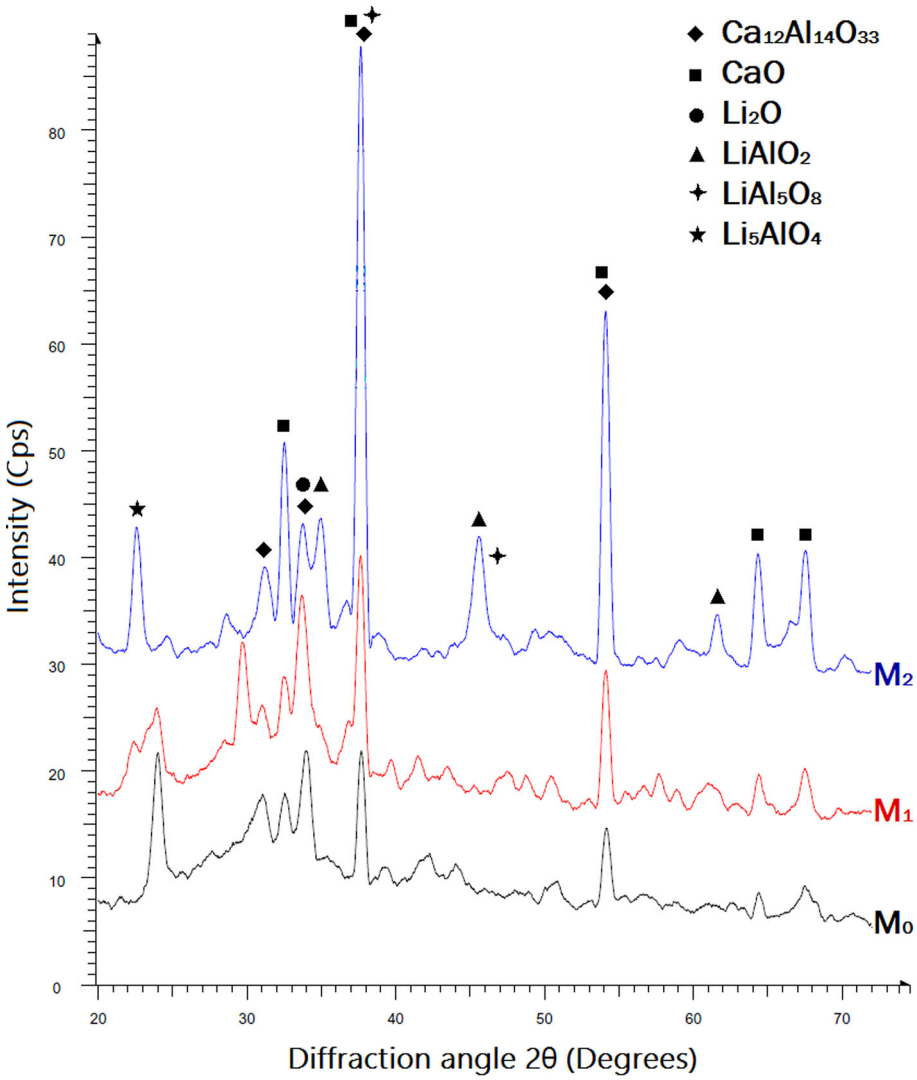

Fig. 2 XRD diffractograms of Li_2O-mayenite catalysts M_0, M_1, and M_2

analysis in Fig. 1, decrease the catalytic activity towards transesterification (catalysts A_4 and A_5 shown in Fig. 6). This reasoning is further strengthened when the BD yield slightly increases in the transesterification using the catalyst A_5 (MgO precipitate/lumps with the impregnated alumina as shown in Fig. 6). The catalysts A_3, A_4, and A_5 might also be at their maximum activity limit regarding their capability for biodiesel production in this conditions as reported by Montero et al. on MgO nanocrystals [75], since the yields are similar between the reactions using the catalysts A_3, A_4, and A_5. However, in the alumina-based catalysts approximately 10% of BD production yield difference shows that Li_2O-alumina (A_1) is the best alumina-based catalyst. High impregnation ratios of MgO or Li_2O affects the catalytic activity in a negative way, while low impregnation ratios increase the catalytic potential surpassing by more than sixfold what bare alumina can provide on its own.

The studies with the mayenite-supported catalysts showed better results reaching maximum conversion with one of the catalysts (M_2). The yields for the different Li_2O-mayenite catalysts (M_1 and M_2) are shown in Fig. 7, from which it can be concluded that the activity increase is exponential with the increasing amount of Li_2O and thus is highly active catalysing triglyceride conversion to biodiesel. Such results are in agreement to previous reports on Li_2O activity for transesterification [25, 47] but on other supports.

The yields with the increasing amount of MgO (M_3 and M_4) show an increase of triglyceride conversion (Fig. 7). However, the activity increase from pure mayenite to 30 wt% of MgO impregnation is not high, from 7.6% BD to 23.6% BD yield, respectively. Such behaviour shows that the impregnation of MgO over mayenite is not very active under these conditions and is in accordance with the literature regarding MgO on other supports [18, 76, 77],

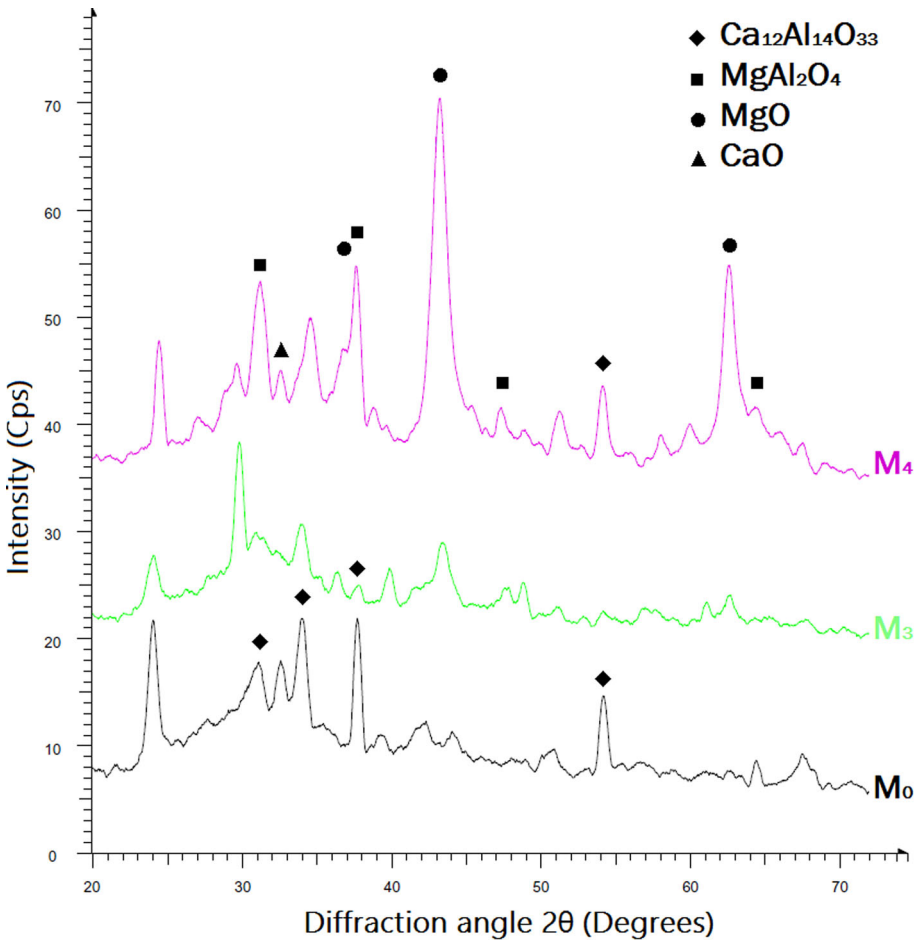

Fig. 3 XRD diffractograms of MgO-mayenite catalysts M_0, M_3, and M_4

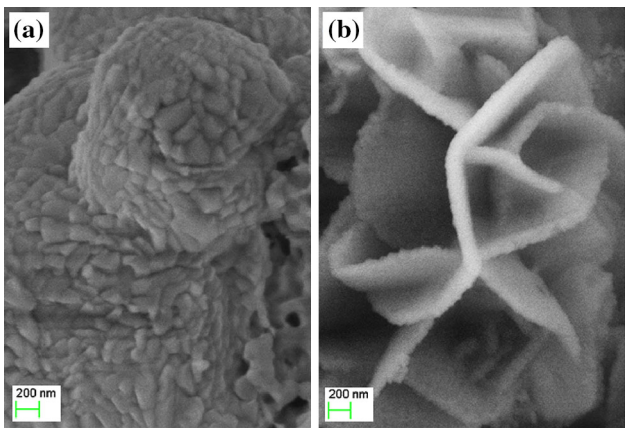

Fig. 4 SEM micrographs of mayenite (**a**) and Li_2O-mayenite (**b**)

suggesting that MgO alone has a relative inferior catalytic activity among the alkaline earth metals.

One important observation from Fig. 7 is that mayenite itself is slightly catalytic for the transesterification reaction. Despite a rather small activity, the BD yield is 8%, such active support characteristics demonstrates a potential of mayenite as a support for the catalysed reaction.

Catalyst concentration in the transesterification

The effect of the catalyst loading was evaluated based on the final BD yields. Batches with varying amounts of catalyst were run using the same reaction conditions. The results from these variations are presented in Figs. 8 and 9.

Mayenite-supported catalysts were used in three different loadings of catalysts in relation to oil mass. The trend for the lithium impregnated catalysts (mayenite with lithium oxide impregnation of 5 and 10%, M_1 and M_2) in the three loadings of catalysts into the reactor (2.5, 5.0, and 10.0 wt%) is quite different (Fig. 8). The first catalyst, which had lower Li_2O impregnation (M_1), had almost constant conversion for the batches with 2.5 and 5.0 wt% of catalyst loaded into the reactor. When increasing the amount up to 10 wt% of M_1 catalyst into the reactor, the yield had no significant increase (27.0% of BD).

The seemingly constant yield between the 2.5 and 5.0 wt% loading of catalysts might be explained by the lack of more active sites, being at the lower limit of catalytic activity. The transesterification reaction occurs due to the reduction of the activation energy of the three consecutive reversible reactions. It has been determined by

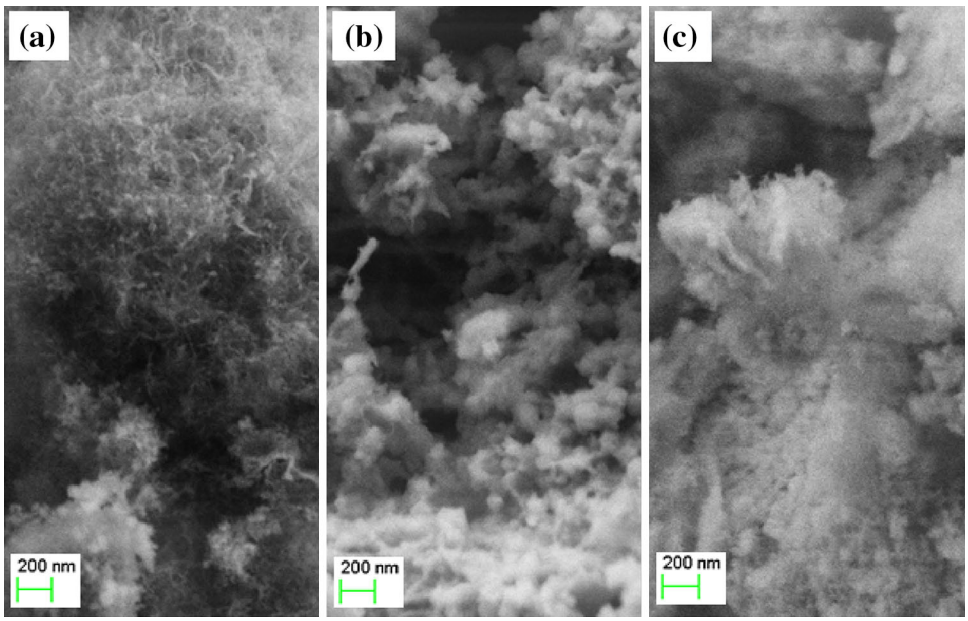

Fig. 5 SEM micrographs of alumina (**a**), Li_2O-alumina (**b**), and MgO-alumina (**c**)

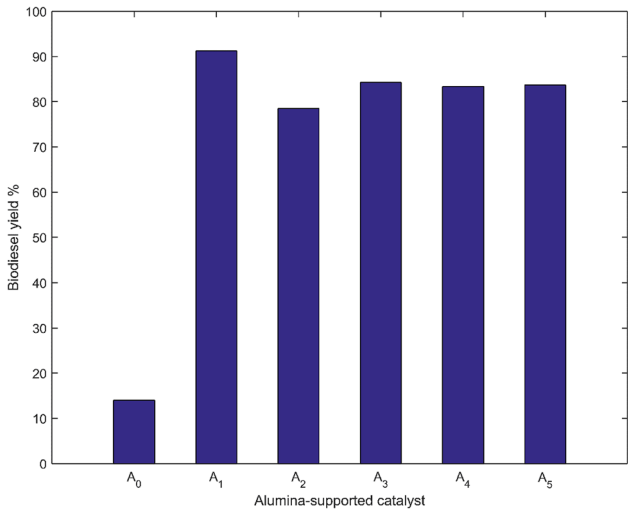

Fig. 6 Biodiesel yields using different alumina-supported catalysts

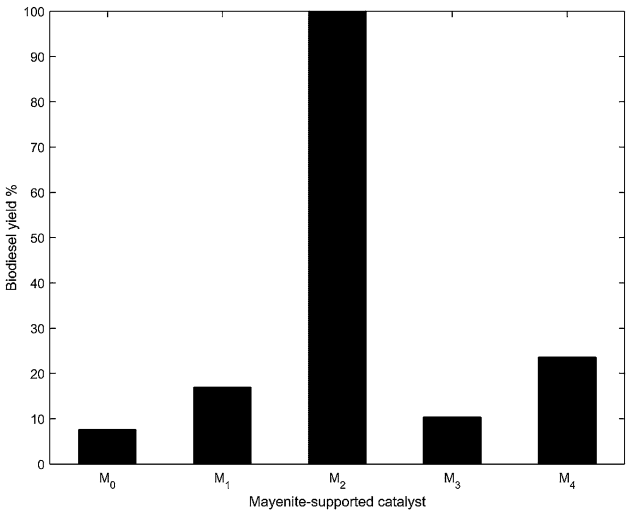

Fig. 7 Biodiesel yields using different mayenite-supported catalysts

other authors that such reduction of the activation energy might be achieved by high reaction conditions (temperature and pressure [53, 78]) as well as by the activity of the catalyst. The reactions to produce diglycerides and monoglycerides from triglycerides can be achieved with the conditions stated above, but the final glycerol production tends to be kinetically slower in the absence of a catalyst. As the catalytic material is relatively low, in the reactions with the loadings of 2.5 and 5.0 wt% into the reactor, the yield will be low as well. The fact that the reaction yield slightly increases by the highest load of catalyst (M_1 at 10 wt% loading into the reactor) suggest that more catalytic material is needed to increase the catalytic sites for the reaction to proceed at higher rates.

The yields of the reactions by M_2 catalyst (Fig. 8) increase between the two lower loadings (2.5 and 5.0 wt%) and then decreases in the last case (10 wt%). The results in Fig. 8 show that Li_2O is a very active specie on the mayenite. The increased concentration of lithium oxide on the mayenite (from 5 to 10 wt% of impregnation) and the support catalysts larger surface properties, give rise to low mass transfer limitations and high triglyceride conversions. The slight drop in BD yield when 10 wt% of the catalyst M_2 is loaded into the reactor suggests that the steady agitation rate—this variable was kept constant at 180 rpm for all the experiments—might affect the reaction environment reducing the turbulent regime in the reactor and leading to an increase of the mass transfer limitations.

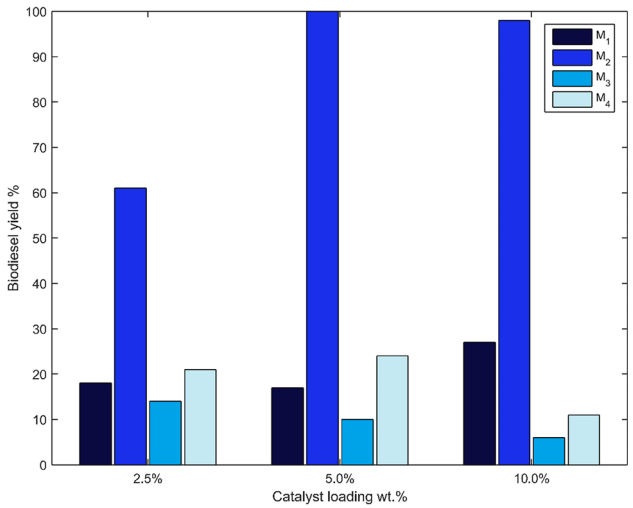

Fig. 8 Loadings of catalysts (M_1 to M_4) for BD production

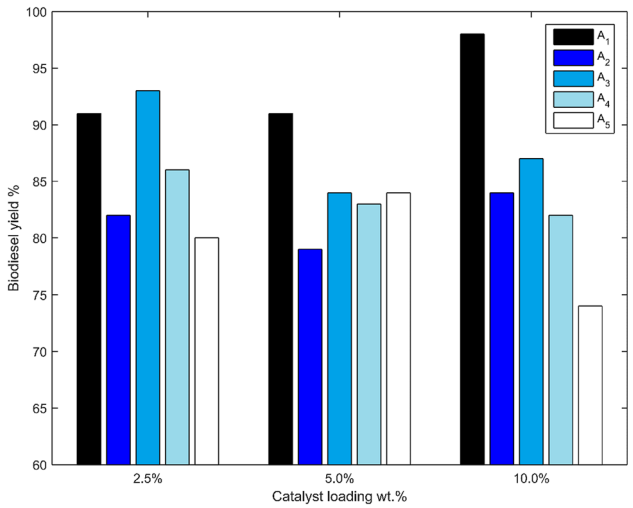

Fig. 9 Loadings of catalysts (A_1 to A_5) for BD production

From Fig. 8 it can be seen that higher yields are generally rendered from the catalysts with a higher level of MgO impregnation (M_3 and M_4). However, when increasing the amount loaded into the reactor, the batches with M_3 drop in yield with increased amount of catalyst. This is not the case for M_4, where the yield first goes up slightly and then levels off to a BD yield of 11% when increasing the catalyst amount in the reactor up to 10 wt%. The reason for this may be the agitation rate, enough to keep the medium in a laminar regime, which increases the mass transfer limitations and results in reduced BD yields. The catalytic activity of MgO 5.0 wt% impregnated over mayenite (M_3) is low as demonstrated by the experiments with 2.5, 5, and 10 wt% of such catalyst into the reactor (Fig. 8). When impregnating with higher concentration of MgO (M_4), the catalytic activity of the catalyst is high enough to enhance the yield slightly when adding more catalyst to the reactor. In the case of mayenite impregnated with 30 wt% MgO (catalyst M_4) the surface area and pore volume increase significantly, which in turn reduces the mass transfer limitations. This would then make the reaction more kinetically controlled [79]. When subsequently increasing the catalyst amount to 10 wt% into the reactor, the yield goes down, probably again due to the mass transfer limitation as a result of the reduced turbulence. The M_4 catalyst had the highest surface area of the mayenite catalysts, making it occupy larger volumes. As a consequence, a 10 wt% catalyst loading into the reactor took up more space than the other catalysts (M_1, M_2, and M_3), decreasing the turbulence in the reactor and causing the reaction to proceed at slower rate.

Analysing the results of the alumina-supported catalysts, it can be seen that for the A_1 catalyst the yields constantly increase with the increasing catalyst amount (Fig. 9). For the higher impregnations of Li_2O (A_2), the yield first drops from the first batch to the second and then finally rises to a yield higher than the initial one (in the range from 2.5 to 10.0 wt% of catalyst load). The trend for A_1 suggests that there is no mass transfer limitation with increasing the amount of catalyst in the reactor, at the same time shows that between 2.5 and 5.0 wt% of catalyst load the yield is not significantly increasing, and at an utterly high amount of catalyst (a catalyst increase from 2.5 to 10.0 wt%) the BD yield has an increase from 91 to 98% BD yield suggesting that the catalyst A_1 is lacking of more active sites to achieve higher BD yields. The trend with catalyst A_2 suggests that there is a mass transfer hindrance at lower catalyst amounts, but when increasing the catalyst amount to 10 wt%, the sheer amount of catalyst makes the yield go up since more active catalytic sites are involved in the reaction.

The alumina-supported catalysts impregnated with MgO are shown in Fig. 9. Starting with A_3, the yield at first is very high, then drops to a level of 84% of BD yield, and then again increases up to 87% of BD yield. The reason for this behaviour of the yields might be due to a poor MgO adsorption over the alumina support. As a result, not all of the MgO is impregnated over the alumina support, and is in a "free state" as MgO powder. When the catalyst was later fed into the reactor, the ratio between MgO-alumina catalyst and MgO powder might have induced such differences showing the instability of the catalysts A_3, A_4, and A_5. The case for the A_4 catalyst shows that the yield continuously drops with increasing amounts of loaded catalyst. Since the MgO particles on alumina have a lower pore volume than the bare alumina, it would lead the mass transfer limitations to occur earlier than in the case with free MgO particles.

The trend of A_5 experiments (catalyst with MgO particles) is that the activity first increases from the lower

catalyst amount to the middle one, only to finally decrease below the value of the initial yield. This also makes sense, considering that probably the mass transfer limitations occurs due to the constant agitation rate instead of adjusting the agitation rate to each catalyst loading in the reactor.

Transesterification kinetics

The reaction rate for a solid phase catalysed transesterification, as suggested by other authors, might evolve through three stages [53, 80]. Initially the conversion rate of BD is fairly low. Considering a three-phase reaction system (methanol, oil, and catalyst), such rate might be due to possible mass transfer limitations, and the time needed to form the reactive methoxide phase over the catalyst surface may delay the BD production, all this followed by a possible pseudo second-order reaction rate on the early stages of the reaction [81]. In the second stage, when the BD production increases, the liquid phase of the reactant mixture might become more uniform and the methoxide complex forms faster in a two-phase reaction system (liquid–solid) leading to an increase in the reaction rate and at this stage the reaction rate has been reported to follow a pseudo-first-order reaction rate [53, 80, 82–86]. The third stage is characterized by a decrease in the reaction rate that occurs due to the oil depletion (triglyceride source).

A mass balance over the reactor is carried out defining the design as a stirred tank reactor batch process, leading to the reaction rate shown in Eq. 1.

$$V_{\mathrm{Cat}} r_{\mathrm{A}} = \frac{\mathrm{d}C_{\mathrm{A}}}{\mathrm{d}t} V_{\mathrm{Tot}} \rightarrow r_{\mathrm{A}} = \frac{\mathrm{d}C_A}{\mathrm{d}t} \frac{V_{\mathrm{Tot}}}{V_{\mathrm{Cat}}} \tag{1}$$

The global reaction obeys Eq. 2 in the presence of a catalyst, where A is the triglyceride; B is the methanol; C is the biodiesel; and D is the glycerol.

$$A + 3{\cdot}B \leftrightharpoons 3{\cdot}C + D \tag{2}$$

Following Eq. 2, the overall conversion should follow a fourth order reaction rate law [84]. The way to steer the reaction towards the fatty acid methyl ester production is to use the methanol in excess. If an excess of methanol is used in the reaction and considering that the second stage of the reaction is predominant (two phase reaction system), it is possible to approximate its overall kinetics to a pseudo-first-order reaction rate by simplifying it as shown in the Eq. 3:

$$r_A = -kC_A C_B^3 \cong -k^* C_A \tag{3}$$

where k^* is the pseudo-first-order rate constant. Replacing Eq. 1 in Eq. 3 for r_{A} and rearranging the terms to have the model relating the variables of concentration to density and mass (Eq. 4):

$$\begin{aligned} \frac{\mathrm{d}C_A}{\mathrm{d}t} = -k^* C_A \rightarrow \ln\left(\frac{C_A}{C_{Ao}}\right) &= -k^* \left(\frac{V_{\mathrm{Cat}}}{V_{\mathrm{Tot}}}\right) t + C \\ &= -k^* \frac{\rho_{\mathrm{Tot}}}{\rho_{\mathrm{Cat}}} \left(\frac{m_{\mathrm{Cat}}}{m_{\mathrm{Tot}}}\right) t + C \end{aligned} \tag{4}$$

Such equation in terms of conversion and suggesting a constant density ratio between the density of the total volume and the density of the catalyst that can be included in the apparent reaction rate constant as k^{**}, will result in (Eq. 5):

$$-\ln(1 - X_A) = k^{**} \frac{m_{\mathrm{Cat}}}{m_{\mathrm{Tot}}} t + C \tag{5}$$

The model in Eq. 5 describes the reaction behaviour, which could be plotted, i.e. $-\ln(1 - X_{\mathrm{A}})$ vs. t, and is used to determine k^{**} having the units min^{-1}.

When observing the yield vs. time plot (Fig. 10), it is clear that initially the reaction is not limited as a three stage system. Instead, the conversion rate is constant for the first 40 min of the reaction. This suggests that enough agitation was used to skip the first stage of the reaction, where the mass transfer limitations have detrimental effects on the reaction rate. The particle size might have aided as well, as a study by Pugnet et al. [87] shows that for catalyst powders with a particle size smaller than 500 μm such mass transfer limitation are avoided. After the initial 40 min, the conversion rate start decreasing and the process reaches the third stage due to the depletion of reactants in the transesterification reaction.

The kinetics were determined on the transesterification reaction with the catalyst M_2 (mayenite plus Li_2O 10 wt%), using a catalyst load of 5 wt% relative to oil, reaction temperature of 60 °C, agitation rate of 180 rpm, a molar ratio of 6:1 (CH_3OH:oil), and a reaction time of 2 h.

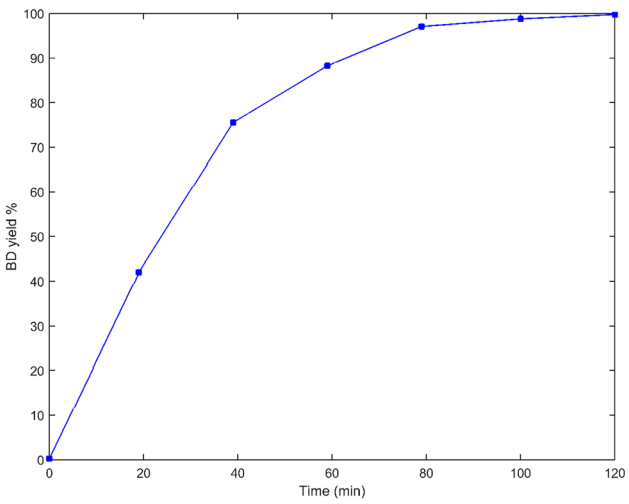

Fig. 10 BD yield plotted against the reaction time in the kinetic study

The reaction rate constant, was obtained by the use of Eq. (5) and plotted as displayed in Fig. 11.

The apparent rate constant (k^{**}) value according to the slope of Fig. 11 was found to be 0.0447 min^{-1}. The R^2 value is nearly 0.97 indicating that the curve fitting is acceptable. Furthermore, the obtained reaction rate expression can be compared with previously reported transesterification kinetic studies. Deshmane and Adewuyi [53] reported a pseudo-first-order reaction rate for homogeneous transesterification that has a reaction rate constant close to the value found in this study ($k^* \approx 0.036\ min^{-1}$). Supported on their study is also possible to confirm that the properties of the catalyst M_2 (mayenite-lithium oxide) enable the possibility to reduce the mass transfer limitation, avoiding the initial delay in the reaction (described as the first stage of the transesterification [53, 80]), and being comparable to a homogeneous transesterification system.

Catalyst reusability

Two different catalysts were selected to study their ability to be reused. The yields of the two different catalysts—M_2 and A_4—are shown in Fig. 12. To prepare the catalysts for reuse tests, they were filtered after one transesterification, to separate them from the reaction mixture, as the glycerol is the by-product of the reaction to which the catalysts are attached for some time. When all the biodiesel had been filtered off the reaction mixture, the catalyst was cleaned with methanol, rendering it ready to be reused.

The alumina catalyst (A_4) did not perform well in the reusability test (Fig. 12) as its catalytic activity dropped to less than half the original value. The catalyst might have been deactivated due to catalytic material loss during the reaction. This experiment also confirms the weak

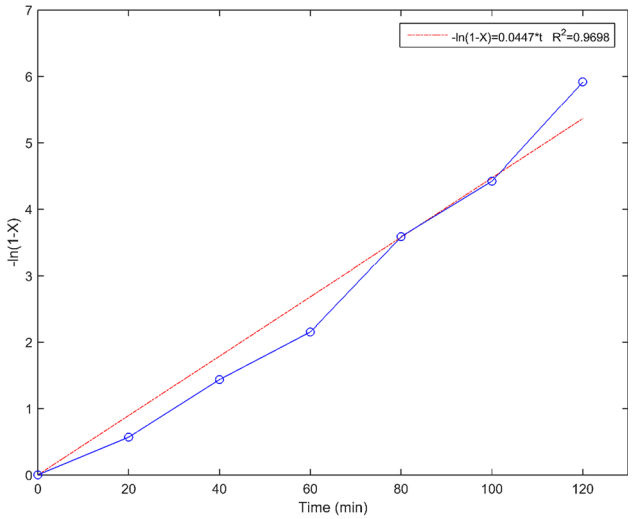

Fig. 11 Reaction rate plot, fit to Eq. (5)

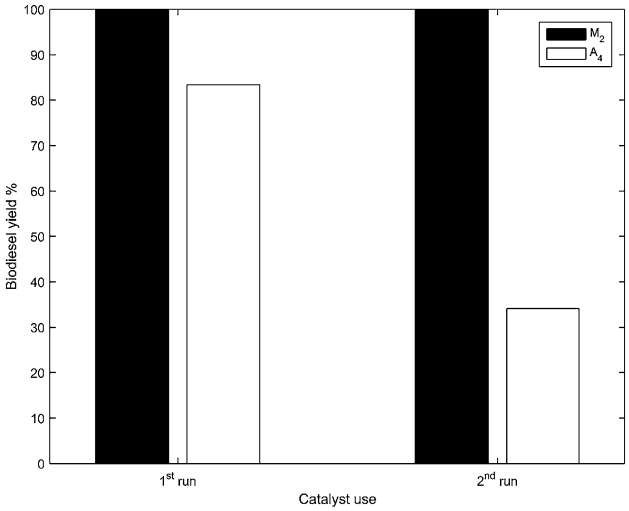

Fig. 12 Catalyst reuse test in terms of BD yield

impregnation of the MgO over alumina and that it was rather a powder surrounding the support, which readily loses the catalytic material in the filtering and washing processes. The filtration of the catalyst M_4 was a slow process due to free MgO particles. This process might also wash away the impregnated MgO making the catalyst lose even more its transesterification activity.

On the other hand, the mayenite-supported catalyst (M_2) showed an outstanding performance for two-cycle reuse transesterification reaction. In both cases the catalyst M_2 was able to achieve a 100% of BD yield. The preparing process for the M_2 catalyst reusability proved to be straightforward since the glycerol and biodiesel were separated from the catalyst with ease. Furthermore, the results of M_2 in this test suggests that Li_2O has been integrated in the mayenite support with the desired material stability. The prospect of reusing the mayenite catalyst (M_2) in more transesterification cycles might hold rather promising results.

Conclusions

Lithium and magnesium oxides were impregnated over alumina and mayenite to be used as catalysts for transesterification reaction of rapeseed oil. The prepared catalyst compositions over such supports were from 5 to 10 wt% and from 5 to 30 wt% of Li_2O and MgO, respectively, producing a total of nine different catalysts. The preparation of the catalysts lead to material with advantageous physical properties of surface area, pore diameter, and pore volume (mesoporous catalysts). The method used to prepare the mayenite-based catalysts in this study was able to increase surface properties when Li_2O was impregnated. The increase of MgO concentration had the same

increasing effect on surface areas while pore diameters were decreased. In the case of alumina-based catalysts, any increase of Li_2O or MgO impregnation concentration led to a decrease of surface area, pore diameter, and pore volume. After the tests of the catalytic activities of the produced catalysts on rapeseed oil transesterification, a series of experiments with different loadings of catalyst in the same reaction conditions were performed. As a result of such experiments, the mayenite-supported catalyst with 5 wt% of impregnated Li_2O (M_2) showed a significantly higher activity compared to other catalysts. The catalyst M_2 showed an increase from 60 to 100% of BD yield, which also showed the advantageous performance over the catalysts supported on alumina (only reaching 96% of BD yield in the best case). Thus, the catalyst M_2 was selected for the reaction kinetics study. The reaction rate experiments showed that the three-phase system (methanol-oil-catalyst) was not controlling the BD production with mayenite-supported catalyst with 5 wt% of impregnated Li_2O. Accordingly, the reaction follows a pseudo-first-order reaction rate with an apparent rate constant of 0.045 min^{-1}. Finally, the reusability tests of the catalysts showed that the catalyst M_2 has potential due to its ability to maintain its complete activity after two cycles.

References

1. Tempels, T.H., Van den Belt, H.: Once the rockets are up, who should care where they come down? The problem of responsibility ascription for the negative consequences of biofuel innovations, SpringerPlus. 5 (2016)
2. Adusumilli, N., Leidner, A.: The U.S. biofuel policy: review of economic and environmental implications. Am. J. Env. Prot. 2, 64–70 (2014)
3. REN21, Renewables 2016 Global status report, Renewable energy policy network for the 21st century. http://www.ren21.net. Accessed 19 May 2016
4. B.E. outlook: Outlook to 2035 (2016). www.bp.com/energyoutlook. Accessed 12 May 2016
5. Rosillo-Calle, F., Pelkmans, L., Walter, A.: A global overview of vegetable oils, with reference to biodiesel. In: Report for the IEA Bioenergy Task Force 40. IEA, Paris (2009)
6. Alasti, P.: Biodiesel process (2009). www.google.com/patents/US7528272. Accessed 20 May 2016
7. Pinto, A.C., Guarieiro, L.L.N., Rezende, M.J.C., Ribeiro, N.M., Torres, E.A., Lopes, W.A., De Pereira, P.A.P., De Andrade, J.B.: Biodiesel: an overview. J. Brazil Chem. Soc. **16**, 1313–1330 (2005)
8. I.C.E. Committees, World agricultural supply and demand estimates, in: U.S.D.o. Agriculture, United States Department of Agriculture, Washington, D.C.40 (2015)
9. Chisti, Y.: Biodiesel from microalgae. Biotechnol. Adv. **25**, 294–306 (2007)
10. Atadashi, I.M., Aroua, M.K., Abdul Aziz, A.R., Sulaiman, N.M.N.: The effects of water on biodiesel production and refining technologies: a review. Renew. Sust. Energy Rev. **16**, 3456–3470 (2012)
11. Mata, T.M., Martins, A.A., Caetano, N.S.: Microalgae for biodiesel production and other applications: a review. Renew. Sust. Energy Rev. **14**, 217–232 (2010)
12. Ma, F., Hanna, M.A.: Biodiesel production: a review. Bioresour. Technol. **70**, 1–15 (1999)
13. Leung, D., Leung, M., Wu, X.: A review on biodiesel production using catalyzed transesterification. Appl. Energy **87**, 1083–1095 (2010)
14. Graboski, M.S., McCormick, R.L.: Combustion of fat and vegetable oil derived fuels in diesel engines. Prog. Energy Combust. **24**, 125–164 (1998)
15. Meher, L.C., Sagar, D.V., Naik, S.N.: Technical aspects of biodiesel production by transesterification—review. Renew. Sust. Energy Rev. **10**, 248 (2006)
16. Borges, M.E., Díaz, L.: Recent developments on heterogeneous catalysts for biodiesel production by oil esterification and transesterification reactions: a review. Renew. Sust. Energy Rev. **16**, 2839–2849 (2012)
17. Islam, A., Taufiq-Yap, Y.H., Chan, E.S., Moniruzzaman, M., Islam, S., Nabi, M.N.: Advances in solid- catalytic and non-catalytic technologies for biodiesel production. Energy Convers. Manage. **88**, 1200–1218 (2014)
18. Endalew, A.K., Kiros, Y., Zanzi, R.: Inorganic heterogeneous catalysts for biodiesel production from vegetable oils. Biomass Bioenerg. **35**, 3787–3809 (2011)
19. Wang, R., Hanna, M.A., Zhou, W., Bhadury, P.S., Chen, Q., Song, B.A., Yang, S.: Production and selected fuel properties of biodiesel from promising non-edible oils: Euphorbia lathyris L., Sapium sebiferum L. and Jatropha curcas L. Bioresour. Technol. **102**, 1194–1199 (2011)
20. Atabani, A.E., Silitonga, A.S., Ong, H.C., Mahlia, T.M.I., Masjuki, H.H., Badruddin, I.A., Fayaz, H.: Non-edible vegetable oils: a critical evaluation of oil extraction, fatty acid compositions, biodiesel production, characteristics, engine performance and emissions production. Renew. Sust. Energy Rev. **18**, 211–245 (2012)
21. Brownbridge, G., Azadi, P., Smallbone, A., Bhave, A., Taylor, B., Kraft, M.: The future viability of algae-derived biodiesel under economic and technical uncertainties. Bioresour. Technol. **151**, 166–173 (2014)
22. Madras, G., Kolluru, C., Kumar, R.: Synthesis of biodiesel in supercritical fluids. Fuel **83**, 2029–2033 (2004)
23. Demirbas, A.: Biodiesel production from vegetable oils via catalytic and non-catalytic supercritical methanol transesterification methods. Prog. Energy Combust. **31**, 466–487 (2005)
24. Atadashi, I.M., Aroua, M.K., Abdul Aziz, A.R., Sulaiman, N.M.N.: The effects of catalysts in biodiesel production: a review. J. Ind. Eng. Chem. **19**, 14–26 (2013)
25. Endalew, A.K., Kiros, Y., Zanzi, R.: Heterogeneous catalysis for biodiesel production from Jatropha curcas oil (JCO). Energy. **36**, 2693–2700 (2011)
26. Sani, Y.M., Daud, W.M.A.W., Abdul Aziz, A.R.: Activity of solid acid catalysts for biodiesel production: a critical review. Appl. Catal. A-Gen. **470**, 140–161 (2014)
27. Trueba, M., Trasatti, S.P.: γ-Alumina as a support for catalysts: a review of fundamental aspects. Eur. J. Inorg. Chem. **2005**, 3393–3403 (2005)
28. Fritz, U.: Ullmann's Encyclopedia of Industrial Chemistry. Wiley, Weinheim (2003)

29. Eliassi, A., Ranjbar, M.: Application of novel gamma alumina nano structure for preparation of dimethyl ether from methanol. Int. J. Nanosci. Nanotech. **10**, 13–26 (2014)
30. Reyes-Carmona, Á., Gianotti, E., Taillades-Jacquin, M., Taillades, G., Rozière, J., Rodríguez-Castellón, E., Jones, D.J.: High purity hydrogen from catalytic partial dehydrogenation of kerosene using saccharide-templated mesoporous alumina supported Pt–Sn. Catal. Today **210**, 26–32 (2013)
31. Teo, S.H., Taufiq-Yap, Y.H., Ng, F.L.: Alumina supported/unsupported mixed oxides of Ca and Mg as heterogeneous catalysts for transesterification of *Nannochloropsis* sp. microalga's oil. Energy Convers. Manage. **88**, 1193–1199 (2014)
32. Islam, A., Taufiq-Yap, Y.H., Chu, C.M., Ravindra, P., Chan, E.S.: Transesterification of palm oil using KF and NaNO3 catalysts supported on spherical millimetric γ-Al2O3. Renew. Energy **59**, 23–29 (2013)
33. Asri, N.P., Machmudah, S., Wahyudiono, Suprapto, Budikarjono, K., Roesyadi, A., Goto, M.: Palm oil transesterification in sub- and supercritical methanol with heterogeneous base catalyst. Chem. Eng. Proc. **72**, 63–67 (2013)
34. Castro, C.S., Ferreti, C., Di Cosimo, J.I., Assaf, J.M.: Support influence on the basicity promotion of lithium-based mixed oxides for transesterification reaction. Fuel **103**, 632–638 (2012)
35. Zhang, X., Ma, Q., Cheng, B., Wang, J., Li, J., Nie, F.: Research on KOH/La-Ba-Al2O3 catalysts for biodiesel production via transesterification from microalgae oil. J. Nat. Gas Chem. **21**, 774–779 (2012)
36. Umdu, E.S., Seker, E.: Transesterification of sunflower oil on single step sol-gel made Al_2O_3 supported CaO catalysts: effect of basic strength and basicity on turnover frequency. Bioresour. Technol. **106**, 178–181 (2012)
37. Anthony, J.W., Bideaux, R.A., Bladh, K.W., Nichols, M.C.: Handbook of Mineralogy. Mineralogical Society of America, Virginia (2003)
38. Boysen, H., Lerch, M., Stys, A., Senyshyn, A.: Structure and oxygen mobility in mayenite ($Ca_{12}Al_{14}O_{33}$): a high-temperature neutron powder diffraction study. Acta Crystallogr. B **63**, 675–682 (2007)
39. Cesário, M.R., Barros, B.S., Courson, C., Melo, D.M.A., Kiennemann, A.: Catalytic performances of Ni–CaO–mayenite in CO2 sorption enhanced steam methane reforming. Fuel Process. Technol. **131**, 247–253 (2015)
40. Proto, A., Cucciniello, R., Genga, A., Capacchione, C.: A study on the catalytic hydrogenation of aldehydes using mayenite as active support for palladium. Catal. Commun. **68**, 41–45 (2015)
41. Campos-molina, Ma. J., Santamaría-González, J., Mérida-Robles, J., Moreno-Tost, R., Albuquerque, M. C. G., Bruque-Gámez, S., Rodríguez-castellón, E., Jiménez-Jópez, A., Maireles-Torres, P.: Base catalysts derived from hydrocalumite for the transesterification of sunflower oil. Energy Fuel. **24**, 979–984 (2010)
42. Kuwahara, Y., Tsuji, K., Ohmichi, T., Kamegawa, T., Mori, K., Yamashita, H.: Transesterifications using a hydrocalumite synthesized from waste slag: an economical and ecological route for biofuel production. Catal. Sci. Technol. **2**, 1842–1851 (2012)
43. Macleod, C.S., Harvey, A.P., Lee, A.F., Wilson, K.: Evaluation of the activity and stability of alkali- doped metal oxide catalysts for application to an intensified method of biodiesel production. Chem. Eng. J. **135**, 63–70 (2008)
44. Lee, A.F., Bennett, J.A., Manayil, J.C., Wilson, K.: Heterogeneous catalysis for sustainable biodiesel production via esterification and transesterification. Chem. Soc. Rev. **43**, 7887–7916 (2014)
45. Lee, D.W., Park, Y.M., Lee, K.Y.: Heterogeneous base catalysts for transesterification in biodiesel synthesis. Catal. Surv. Asia **13**, 63–77 (2009)
46. Benjapornkulaphong, S., Ngamcharussrivichai, C., Bunyakiat, K.: Al_2O_3-supported alkali and alkali earth metal oxides for transesterification of palm kernel oil and coconut oil. Chem. Eng. J. **145**, 468–474 (2009)
47. Kaur, M., Ali, A.: Lithium ion impregnated calcium oxide as nano catalyst for the biodiesel production from karanja and jatropha oils. Renew. Energy **36**, 2866–2871 (2011)
48. Castro, C., Cardoso, D., Nascente, P., Assaf, J.: MgAlLi mixed oxides derived from hydrotalcite for catalytic transesterification. Catal. Lett. **141**, 1316–1323 (2011)
49. Kumar, D., Ali, A.: Nanocrystalline lithium ion impregnated calcium oxide as heterogeneous catalyst for transesterification of high moisture containing cotton seed oil. Energy Fuel. **24**, 2091–2097 (2010)
50. Ding, Y., Sun, H., Duan, J., Chen, P., Lou, H., Zheng, X.: Mesoporous Li/ZrO_2 as a solid base catalyst for biodiesel production from transesterification of soybean oil with methanol. Catal. Commun. **12**, 606–610 (2011)
51. Lu, H., Yu, X., Yang, S., Yang, H., Tu, S.T.: MgO–Li_2O catalysts templated by a PDMS–PEO comb-like copolymer for transesterification of vegetable oil to biodiesel. Fuel **165**, 215–223 (2016)
52. Umdu, E.S., Tuncer, M., Seker, E.: Transesterification of nannochloropsis oculata microalga's lipid to biodiesel on Al_2O_3 supported CaO and MgO catalysts. Bioresour. Technol. **100**, 2828–2831 (2009)
53. Deshmane, V.G., Adewuyi, Y.G.: Synthesis and kinetics of biodiesel formation via calcium methoxide base catalyzed transesterification reaction in the absence and presence of ultrasound. Fuel **107**, 474–482 (2013)
54. Singh, D., Bhoi, R., Ganesh, A., Mahajani, S.: Synthesis of biodiesel from vegetable oil using supported metal oxide catalysts. Energy Fuel. **28**, 2743–2753 (2014)
55. Boz, N., Kara, M.: Solid base catalyzed transesterification of canola oil. Chem. Eng. Commun. **196**, 80–92 (2008)
56. Xiao, Y., Gao, L., Xiao, G., Lv, J.: Kinetics of the transesterification reaction catalyzed by solid base in a fixed- bed reactor. Energy Fuel. **24**, 5829–5833 (2010)
57. Varma, M.N., Sonawane, S.S.: Ultrasound assisted two-stage biodiesel synthesis from non-edible Schleichera triguga oil using heterogeneous catalyst: kinetics and thermodynamic analysis. Ultrason. Sonochem. **29**, 288–298 (2016)
58. Ahmad, A.L., Yasin, N.H.M., Derek, C.J.C., Lim, J.K.: Kinetic studies and thermodynamics of oil extraction and transesterification of Chlorella sp. for biodiesel production. Environ. Technol. **35**, 891–897 (2014)
59. Alba-Rubio, A.C., Santamaría-González, J., Mérida-Robles, J.M., Moreno-Tost, R., Martín-Alonso, D., Jiménez-López, A., Maireles-Torres, P.: Heterogeneous transesterification processes by using CaO supported on zinc oxide as basic catalysts. Catal. Today **149**, 281–287 (2010)
60. Viriya-Empikul, N., Krasae, P., Nualpaeng, W., Yoosuk, B., Faungnawakij, K.: Biodiesel production over Ca- based solid catalysts derived from industrial wastes. Fuel **92**, 239–244 (2012)
61. Ong, H.C., Silitonga, A.S., Masjuki, H.H., Mahlia, T.M.I., Chong, W.T., Boosroh, M.H.: Production and comparative fuel properties of biodiesel from non-edible oils: Jatropha curcas, Sterculia foetida and Ceiba pentandra. Energy Convers. Manage. **73**, 245–255 (2013)
62. Choudhury, H.A., Goswami, P.P., Malani, R.S., Moholkar, V.S.: Ultrasonic biodiesel synthesis from crude Jatropha curcas oil with heterogeneous base catalyst: mechanistic insight and statistical optimization. Ultrason. Sonochem. **21**, 1050–1064 (2014)
63. Li, C., Hirabayashi, D., Suzuki, K.: Synthesis of higher surface area mayenite by hydrothermal method. Mater. Res. Bull. **46**, 1307–1310 (2011)

64. Ruszak, M., Inger, M., Witkowski, S., Wilk, M., Kotarba, A., Sojka, Z.: Selective N2O removal from the process gas of nitric acid plants over ceramic 12CaO 7Al2O3 catalyst. Catal. Lett. **126**, 72–77 (2008)
65. Kouzu, M., Kasuno, T., Tajika, M., Sugimoto, Y., Yamanaka, S., Hidaka, J.: Calcium oxide as a solid base catalyst for transesterification of soybean oil and its application to biodiesel production. Fuel **87**, 2798–2806 (2008)
66. Jiang, P., Lu, G., Guo, Y., Guo, Y., Zhang, S., Wang, X.: Preparation and properties of a γ-Al_2O_3 washcoat deposited on a ceramic honeycomb. Surf. Coat. Tech. **190**, 314–320 (2005)
67. Paglia, G., Buckley, C. E., Rohl, A. L., Hart, R. D., Winter, K., Studer, A., Hunter, B.A., Hanna, J.: Boehmite derived gamma-alumina system. 1. Structural evolution with temperature, with the identification and structural determination of a new transition phase, gamma-alumina. Chem. Mat. **16**, 220–236 (2004)
68. Huang, H., Wang, L., Cai, Y., Zhou, C., Yuan, Y., Zhang, X., Wan, H., Guan, G.: Facile fabrication of urchin-like hollow boehmite and alumina microspheres with a hierarchical structure via Triton X-100 assisted hydrothermal synthesis. Cryst. Eng. Comm. **17**, 1318–1325 (2015)
69. Chien, W.M., Chandra, D., Lamb, J.H.: X-ray diffraction studies of Li-based complex hydrides after pressure cycling. Adv. X-Ray Anal. **51**, 190–195 (2008)
70. Cheng, J., Guo, L., Xu, S., Zhang, R., Li, C.: Submicron γ-$LiAlO_2$ powder synthesized from boehmite. Chin. J. Chem. Eng. **20**, 776–783 (2012)
71. Lee, J.J., Choi, H.J., Hyun, S.H., Im, H.C.: Characteristics of aluminum-reinforced γ-$LiAlO_2$ matrices for molten carbonate fuel cells. J. Power Sources **179**, 504–510 (2008)
72. Kwon, S., Kim, E., Park, S.: The formation of phase pure lithium aluminate from the bulky lithium and aluminum alkoxides. J. Mater. Sci. Lett. **18**, 931–933 (1999)
73. Li-Zhai, P., Wan-Yun, Y., Ji-Fen, W., Jun, C., Chuan-Gang, F., Qian-Feng, Z.: Low temperature synthesis of magnesium oxide and spinel powders by a sol-gel process. Mater. Res. **13**, 339–343 (2010)
74. Ganesh, I., Bhattacharjee, S., Saha, B.P., Johnson, R., Rajeshwari, K., Sengupta, R., Ramana Rao, M.V., Mahajan, Y.R.: An efficient $MgAl_2O_4$ spinel additive for improved slag erosion and penetration resistance of high-Al_2O_3 and MgO–C refractories. Ceram. Int. **28**, 245–253 (2002)
75. Montero, J.M., Gai, P., Wilson, K., Lee, A.F.: Structure-sensitive biodiesel synthesis over MgO nanocrystals. Green Chem. **11**, 265–268 (2009)
76. Zabeti, M., Wan Daud, W.M.A., Aroua, M.K.: Activity of solid catalysts for biodiesel production: a review. Fuel Process. Technol. **90**, 770–777 (2009)
77. D'Cruz, A., Kulkarni, M., Meher, L., Dalai, A.: Synthesis of Biodiesel from canola oil using heterogeneous base catalyst. J. Am. Oil Chem. Soc. **84**, 937–943 (2007)
78. Anikeev, V., Stepanov, D., Ermakova, A.: Calculating the thermodynamic characteristics of the stepwise transesterification of simple triglycerides. Russ. J. Phys. Chem. **85**, 2082–2087 (2011)
79. Allain, F., Portha, J.F., Girot, E., Falk, L., Dandeu, A., Coupard, V.: Estimation of kinetic parameters and diffusion coefficients for the transesterification of triolein with methanol on a solid $ZnAl_2O_4$ catalyst. Chem. Eng. J. **283**, 833–845 (2016)
80. Veljković, V.B., Stamenković, O.S., Todorović, Z.B., Lazić, M.L., Skala, D.U.: Kinetics of sunflower oil methanolysis catalyzed by calcium oxide. Fuel **88**, 1554–1562 (2009)
81. Darnoko, D., Cheryan, M.: Kinetics of palm oil transesterification in a batch reactor. J. Am. Oil Chem. Soc. **77**, 1263–1267 (2000)
82. Freedman, B., Butterfield, R., Pryde, E.: Transesterification kinetics of soybean oil. J. Am. Oil Chem. Soc. **63**, 1375–1380 (1986)
83. Singh, A.K., Fernando, S.D.: Reaction kinetics of soybean oil transesterification using heterogeneous metal oxide catalysts. Chem. Eng. Technol. **30**, 1716–1720 (2007)
84. Vujicic, D., Comic, D., Zarubica, A., Micic, R., Boskovic, G.: Kinetics of biodiesel synthesis from sunflower oil over CaO heterogeneous catalyst. Fuel **89**, 2054–2061 (2010)
85. Kaur, N., Ali, A.: Kinetics and reusability of Zr/CaO as heterogeneous catalyst for the ethanolysis and methanolysis of Jatropha crucas oil. Fuel Process. Technol. **119**, 173–184 (2014)
86. Jain, S., Sharma, M.P.: Kinetics of acid base catalyzed transesterification of Jatropha curcas oil. Bioresour Technol. **101**, 7701–7706 (2010)
87. Pugnet, V., Maury, S., Coupard, V., Dandeu, A., Quoineaud, A.A., Bonneau, J.L., Tichit, D.: Stability, activity and selectivity study of a zinc aluminate heterogeneous catalyst for the transesterification of vegetable oil in batch reactor. Appl. Catal. A-Gen. **374**, 71–78 (2010)